Ultrastructural Localization of Nitrotyrosine within the Caudate-Putamen Nucleus and the Globus Pallidus of Normal Rat Brain

Elizabeth A. Bolan,[1] K. Noelle Gracy,[2] June Chan,[2] Rosario R. Trifiletti,[3] and Virginia M. Pickel[3]

Departments of [1]Pharmacology, [2]Neurology and Neuroscience, and [3]Pediatric Neurology, Weill Medical College of Cornell University, New York, New York 10021

Nitration of protein tyrosine residues by nitric oxide (NO)-derived reactive species results in the production of stable nitrotyrosine (NT) moieties that are immunochemically detectable in many regions of normal brain and enriched in those areas containing constitutive nitric oxide synthase (cNOS). These include the caudate-putamen nucleus (CPN) and the globus pallidus, which receives major inhibitory input from the CPN. To determine the functional sites for NT production in these critical motor nuclei, we examined the electron microscopic immunocytochemical localization of NT and cNOS in rat brain. In the CPN, NT was localized to the somata and dendrites of cNOS-containing interneurons and spiny neurons, some of which received input from cNOS-labeled terminals. The NT immunoreactivity was most prevalent on outer mitochondrial membranes and nearby segments of the plasma membranes in dendrites and within asymmetric synapses on dendritic spines. In the CPN and globus pallidus, there was also a prominent labeling of NT in astrocytic processes, small axons, and tubulovesicles and/or synaptic vesicles in axon terminals. These terminals formed mainly asymmetric synapses in the CPN and inhibitory-type synapses in the globus pallidus where they often apposed cNOS-containing terminals that also formed asymmetric, excitatory-type synapses. Our results suggest that NT is generated by mechanisms requiring the dual actions of excitatory transmitters and NO derived either from interneurons in the CPN or from excitatory afferents in the globus pallidus. The findings also implicate NT in the physiological actions of NO within the striatal circuitry and, particularly, in striatopallidal neurons severely affected in Huntington's disease.

Key words: nitric oxide synthase; nitric oxide; motor function; plasticity; neurodegeneration; subthalamic nucleus

The highly reactive species peroxynitrite is formed via the near diffusion-limited reaction of nitric oxide with superoxide free radicals (van der Vliet et al., 1995, 1996; Dalton et al., 1999). Peroxynitrite is a potent oxidant that can react with a variety of biological molecules producing nitration of phenolic rings, predominantly in the *ortho* position of tyrosine residues, which leads to the formation of 3-nitrotyrosyl moieties (Ohshima et al., 1990; Ischiropoulos et al., 1992). These stable 3-nitrotyrosyl residues are readily detectable in fixed and fresh tissues by a variety of techniques including specific affinity-purified polyclonal and monoclonal antibodies, amino acid analysis, HPLC analysis, and gas chromatography/mass spectrometry (Crow and Ischiropoulos, 1996; Ischiropoulos et al., 1996).

Peroxynitrite formation is markedly enhanced in many neurodegenerative disorders, leading to the possibility that peroxynitrite is either not formed or effectively scavenged in normal tissues (Dawson and Dawson, 1996). More recently, however, we have shown that nitrotyrosine (NT), a relatively stable marker for peroxynitrite production (Ischiropoulos et al., 1992), is not only present in normal adult and developing brain but also is seen in somewhat higher levels in brain regions enriched in constitutive nitric oxide synthase (cNOS)-containing neurons (Bredt et al., 1991; Dawson et al., 1991), including the caudate-putamen nucleus (CPN) (Trifiletti et al., 1995a,b). Immunochemically detectable NT also was present, however, in the globus pallidus and several other brain regions containing few cNOS-immunoreactive somata. In regions without cNOS-containing neurons, the most probable source of NO is afferent projections from neurons that contain cNOS, and in the globus pallidus, these afferents most likely originate in the subthalamic nuclei (Nisbet et al., 1994). In the present study, we examined the dual electron microscopic localization of NT and cNOS in the CPN and globus pallidus of normal rat brain. We show a selective subcellular distribution of NT in cNOS-containing aspiny neurons and in spiny neurons and their excitatory afferents in the CPN and mainly in inhibitory-type terminals in the globus pallidus.

Received Feb. 22, 2000; revised April 10, 2000; accepted April 12, 2000.

This work was supported by National Institutes of Health Grants MH 00078, MH 48776, MH 40342, and HL 18974 to V.M.P. and NS 35184 to R.R.T.

Correspondence should be addressed to Dr. Virginia M. Pickel, Department of Neurology and Neuroscience, Cornell University Weill Medical College, 411 East 69th Street, Kips Bay 410, New York, NY 10021. E-mail: vpickel@mail.med.cornell.edu.

MATERIALS AND METHODS

Antisera. Rabbit polyclonal antiserum recognizing nitrotyrosine residues was raised against nitrated keyhole limpet hemocyanin using previously described methods (Ye et al., 1996). This antiserum was purchased from Upstate Biotechnology (Lake Placid, NY). Two-dimensional gel analysis of striatal homogenates showed a recognition of >50 nitrated protein bands, which is consistent with the many different nitroproteins that are present in brain homogenates (Beckman et al., 1994).

As a control for antibody specificity, immunocytochemistry was also performed using anti-NT serum that had been preadsorbed with 10 mg/ml nitrated bovine serum albumin (BSA) and showing no immunolabeling with either peroxidase or gold methods. Nitrated BSA was prepared in a double chamber consisting of an outer large (1.5 ml) and an inner small (0.5 ml) microcentrifuge tube. Gas was generated in the large tube by combining 100 μl of 1 M nitrite and 100 μl of 1 M phosphoric acid. The nascent gas was allowed to pass to the inner chamber containing 50 μl of 10 mg/ml BSA through holes punched with an 18 gauge syringe at a level above the BSA solution. The lid of the outer chamber was sealed with Parafilm (American National Can, Neenah, WI), and the

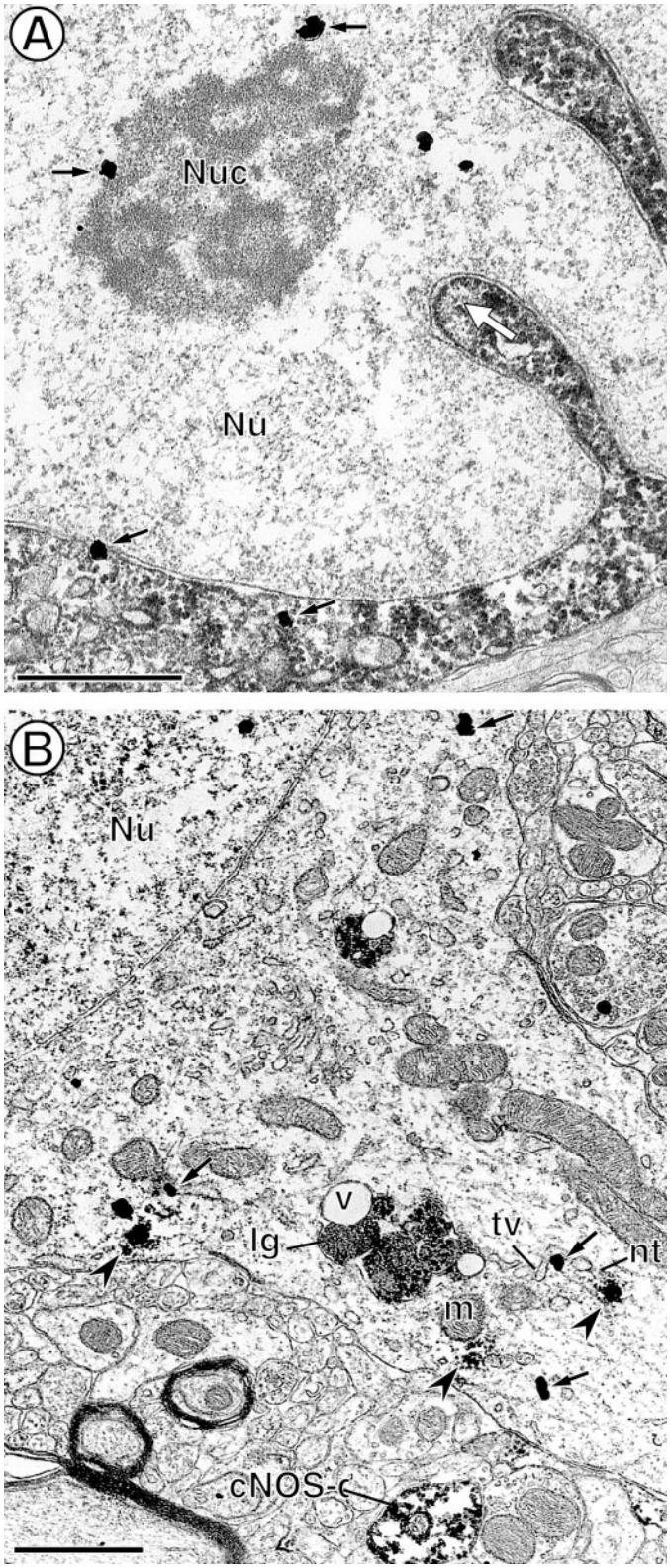

Figure 1. Electron micrographs showing somatic immunogold labeling for NT and immunoperoxidase labeling of cNOS in rat CPN. *A*, NT-immunogold particles (*small black arrows*) are seen within the cytoplasm and nucleus of a somata containing cytoplasmic peroxidase reaction product (*black precipitate*) for cNOS. The gold particles are seen on or near the limiting membrane of the nucleus (*Nu*) that has a large indentation (*large white arrow*). The particles are also distributed within the nuclear matrix near a prominent nucleolus (*Nuc*). *B*, NT-immunogold particles (*arrows*) are seen within the cytoplasm and nucleus (*Nu*) of a somata having an unindented nuclear membrane. The cytoplasmic gold particles contact neurotubules (*nt*), tubulovesicles (*tv*), and mitochondria (*m*) that are located near lipofuscin granules (*lg*) with associated vacuoles (*v*). Within the neuropil, peroxidase labeling for cNOS is also seen in a neuronal process (*cNOS*). Scale bars, 0.5 μm.

reaction continued for 5 min, during which the BSA solution was agitated with a micro stir bar.

A commercial mouse monoclonal antiserum was raised against neuronal (type I) cNOS (Transduction Laboratories, Lexington, KY). The antiserum was generated from human cNOS and shown to recognize selectively a 155 kDa protein from the rat pituitary in Western blots at a 1:2500 dilution. This antiserum has been used previously for light (Pickel et al., 1999) and electron microscopic localization of cNOS in rat forebrain (Gracy and Pickel, 1997).

Animals and tissue preparation. Six adult male Sprague Dawley rats (200–250 gm; Taconic, Germantown, NY) were anesthetized with pentobarbital (100 mg/kg, i.p.) in accordance with the recommendations of the Animal Use Committee at Cornell University Weill Medical College and the National Institutes of Health guidelines for the humane treatment of animals. The brains were fixed by aortic arch perfusion with either (1) 4% paraformaldehyde (200 ml) or (2) 50 ml of a mixture containing 3.75% acrolein and 2% paraformaldehyde in 0.1 M phosphate buffer (PB), pH 7.4. The acrolein–paraformaldehyde solution was followed by 200 ml of 2% paraformaldehyde (Leranth and Pickel, 1989). The brains were sectioned rostrocaudally through the region of the CPN and globus pallidus at a thickness of 40 μm on a vibrating microtome. The area was identified using a rat brain atlas (Paxinos and Watson, 1986). To enhance penetration of immunoreagents, the vibratome sections were washed in PBS, placed in a cryoprotectant, and freeze-thawed. Triton X-100 (0.0035%) was also used in some of the antisera incubations to enhance antibody penetration. Use of the detergent appeared to enhance detected NT immunoreactivity but produced damaged membranes, resulting in limited use for electron microscopy.

Immunolabeling. For single peroxidase labeling of NT, the vibratome sections were incubated overnight at room temperature, or for 48 hr at 4°C, in a rabbit NT antiserum at a 1:1000 dilution. After the primary incubation, the sections were rinsed and incubated for 30 min in goat anti-rabbit biotinylated IgG (1:400; Sigma, St. Louis, MO). The peroxidase was visualized by reacting sections for 6 min in 3,3′-diaminobenzidine (DAB; Aldrich, Milwaukee, WI).

For single gold–silver labeling of NT, the sections of tissue were incubated overnight in the NT antiserum at a 1:500 dilution. After a buffer rinse, these sections were placed for 30 min in a 1:50 dilution of goat anti-rabbit IgG (Amersham, Arlington Heights, IL) that was bound to 1 nm colloidal gold particles. The gold particles were enlarged for microscopic analysis by silver intensification using the IntenS-EM kit (Amersham) as described by Chan et al. (1990).

The above methods were combined (Chan et al., 1990) for dual labeling of NT and cNOS. The sections were incubated in rabbit anti-NT (1:1000 dilution) and mouse anti-cNOS (1:50) antisera for 48 hr at 4°C. The tissue was processed using goat anti-rabbit biotinylated IgG, the Vector Elite ABC kit (Vector Laboratories, Burlingame, CA), and DAB to visualize the rabbit NT antiserum. This was followed by a 2 hr incubation with a 1:50 dilution of rabbit anti-mouse 1 nm colloidal gold IgG (Amersham) and silver enhancement to visualize the mouse cNOS antiserum. The gold and peroxidase labels were reversed to demonstrate the presence of a similar distribution in labeling between the two methods. The second set was incubated for 2 hr with a 1:400 dilution of rabbit anti-mouse biotinylated IgG and processed using the Vector Elite ABC kit and DAB to visualize the mouse cNOS antiserum. After the DAB reaction, these sections were placed for 2 hr in a 1:50 dilution of goat anti-rabbit 1 nm colloidal gold IgG, followed by silver enhancement of the gold particles for detection of the rabbit NT antiserum. Control experiments included processing the tissue for dual labeling with omission of one antiserum in each set to test for potential cross-species interactions.

Microscopic examination and nomenclature. Immunolabeled vibratome sections through the CPN and globus pallidus from each of the animals were processed for light or electron microscopy. For light microscopy, the sections were mounted on glass slides, dehydrated, and covered with a glass coverslip. These slides were examined with a Nikon microscope

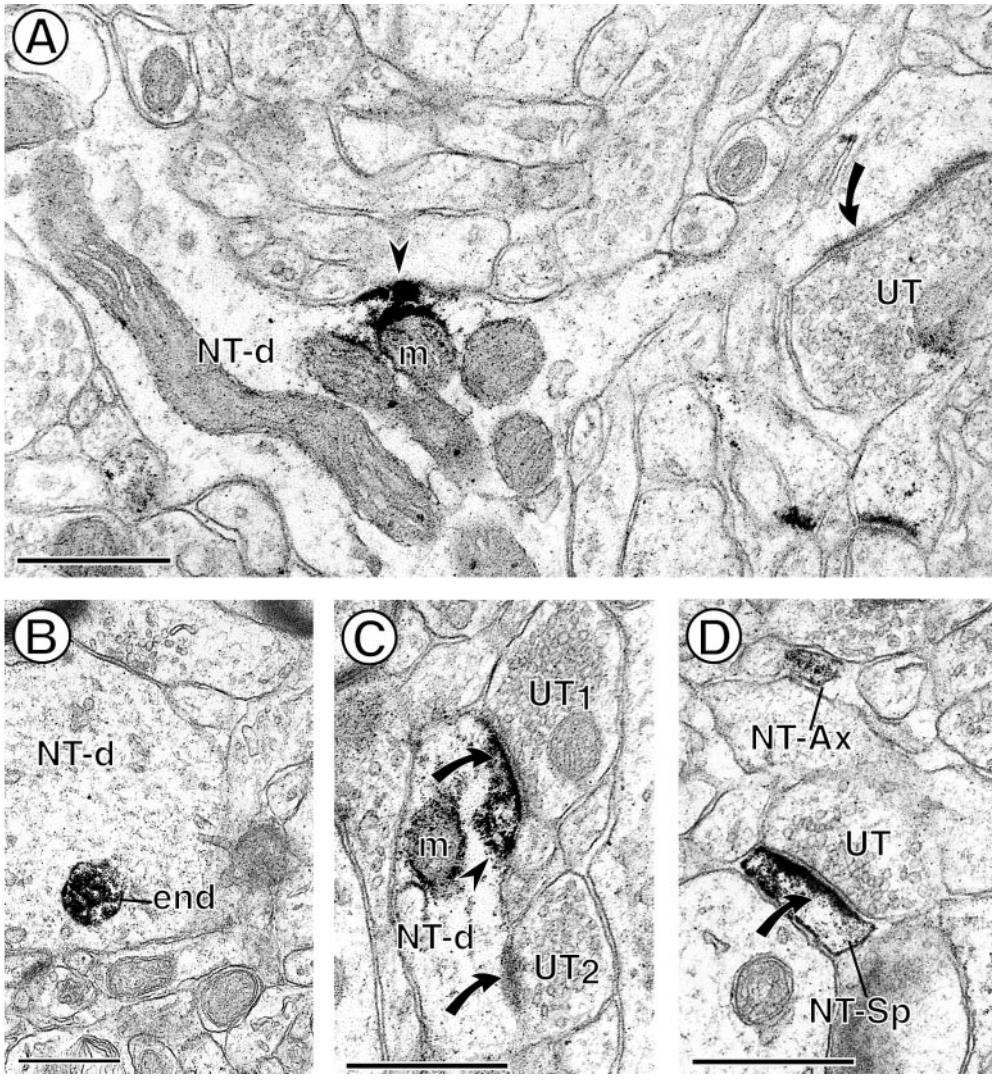

Figure 2. Immunoperoxidase labeling for NT in dendrites in the CPN. *A*, The peroxidase reaction product (*arrowhead*) is seen along the plasma membrane and within the cytoplasm near several large mitochondria (*m*) of a spiny dendrite (*NT-d*). The spine head seen in continuity with the NT-immunoreactive dendrite is unlabeled and receives a perforated asymmetric synapse (*curved arrow*) from an unlabeled axon terminal (*UT*). *B*, Localization of NT labeling within an endosome-like organelle (*end*) in a dendrite (*NT-d*) is shown. *C*, The NT-peroxidase reaction product (*arrowhead*) is seen within and near an asymmetric synapse (*top curved arrow*) formed by an unlabeled terminal (UT_1) but absent from a similar synapse (*bottom curved arrow*) that is formed by another unlabeled terminal (UT_2). This NT-labeled dendrite (*NT-d*) also contains a mitochondrion (*m*) showing NT immunoreactivity along its outer membrane. *D*, Immunoperoxidase labeling for NT within a dendritic spine (*NT-Sp*) that receives an asymmetric synapse (*curved arrow*) from an unlabeled terminal (*UT*) is shown. A small axon (*NT-Ax*) also shows peroxidase labeling for NT within the neuropil. Scale bars, 0.5 μm.

using bright-field and differential interference optics. For electron microscopy, the sections were rinsed in 0.01 M PBS and then fixed for 1 hr in 2% osmium tetroxide in PBS, dehydrated, and flat-embedded in Epon 812. Ultrathin sections were collected from the outer surface of the plastic-embedded tissues at the level of the midcaudal CPN and globus pallidus, as defined by the atlas of Paxinos and Watson (1986). These were placed on copper mesh grids, counterstained with uranyl acetate and Reynolds lead citrate (Reynolds, 1963), and examined using a Philips CM10 electron microscope. Electron micrographs that were used for illustrations were scanned on a Power Macintosh 8500/150 Computer (Apple Computer, Cupertino, CA) with an Agfa Arcus II scanner (Agfa-Gevaert) in combination with FotoLook (Agfa-Gevaert) and Photoshop software (version 3.0.4; Adobe Systems, Mountain View, CA). QuarkX-Press (version 3.32; Quark, Denver, CO) and Adobe Illustrator (version 6.0; Adobe Systems) software were used to prepare and label the composite figures.

Neuronal and glial profiles were identified on the basis of descriptions by Peters et al. (1991). We defined neuronal somata as neuronal profiles containing nuclei and receiving input from unlabeled terminals, whereas dendrites contained similar cytoplasmic organelles and also usually received synaptic input from axon terminals. Neuronal profiles were classified as small unmyelinated axons if they were 0.1–0.25 μm in cross-sectional diameter and contained neurotubules and/or small vesicles. Axon terminals were defined as elements 0.25 μm or larger in diameter and containing numerous small synaptic vesicles (SSVs). Axon terminals were defined as forming asymmetric synapses when their postsynaptic densities were thicker than the presynaptic junctions but as symmetric synapses when these membranes appeared equally electron dense. Glia were defined by their irregular profiles and by astrocytic filaments (Peters et al., 1991).

RESULTS

Light microscopy showed a limited and diffuse distribution of nitrotyrosine-like immunoreactivity (NT-LI) throughout the CPN and globus pallidus, as well as in the overlying cerebral cortex. A distinct neuronal and glial distribution of NT-LI was seen, however, by electron microscopy in each region, suggesting that the diffuse light microscopic labeling was primarily attributed to a subcellular localization within structures below the resolution of the light microscope. There were no observable differences in the light microscopic density of NT labeling in brain tissue fixed by vascular perfusion using paraformaldehyde as compared with acrolein, which could potentially reduce a protein-bound nitro group to an amine (King et al., 1983). The NT-LI as seen by either light or electron microscopy was markedly reduced by preadsorption of the primary antiserum with nitrated BSA and was absent in sections processed without the primary antiserum.

In the dorsolateral CPN, NT-LI was observed in the somata and dendrites of neurons having the features of aspiny and spiny neurons, the former of which were often cNOS immunoreactive. In this region, axon terminals forming mainly asymmetric syn-

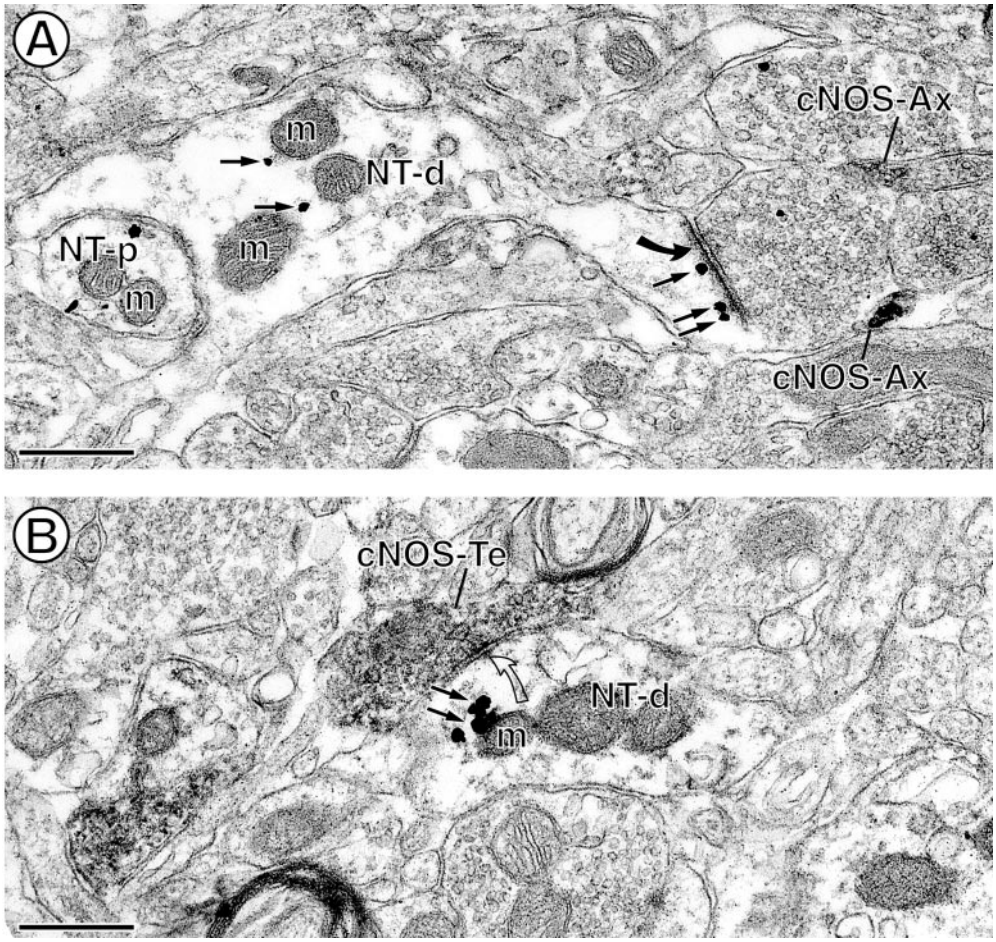

Figure 3. Differential distributions of NT and cNOS in the CPN. *A*, Immunogold NT labeling (*small black arrows*) is seen within the postsynaptic density formed by an axon terminal that apposes small axons that contain cNOS immunoperoxidase labeling (*cNOS-Ax*). The dendrite (*NT-d*) also shows immunogold NT labeling (*small black arrows*) near two mitochondria (*m*). An apposed process (*NT-P*) also contains NT-immunogold particles and mitochondria. *B*, Immunogold labeling for NT (*small black arrows*) is seen near a mitochondrion (*m*) in a dendrite (*NT-d*) that receives a symmetric synapse (*large white curved arrow*) from an axon terminal containing diffuse peroxidase labeling for cNOS (*cNOS-Te*). Scale bars, 0.5 μm.

apses also contained NT-LI. These axon terminals usually were without detectable cNOS but were sometimes located near other neuronal profiles containing this enzyme. Many axons in the CPN, as well as in the globus pallidus, also contained NT-LI. Small axons and/or small glial processes comprised 58% of the total of 1063 NT-labeled profiles that were observed in the globus pallidus. The other profiles were mainly axon terminals (26%) or larger, more clearly defined astrocytic processes (12%). Somata and dendrites constituted the remaining NT-labeled profiles.

Cellular distribution of NT in the CPN

Somata and dendrites

NT-LI was localized within somata having indented nuclei (Fig. 1*A*) that are typical of aspiny neurons (DiFiglia et al., 1980) and in those containing round unindented nuclei (Fig. 1*B*), which are characteristic of spiny projection neurons (DiFiglia et al., 1980). Many of the NT-labeled aspiny somata (Fig. 1*A*) and their proximal dendrites contained intense cNOS immunoreactivity. In contrast, spiny somata and dendrites containing NT were usually without cNOS immunoreactivity, although isolated patches of cNOS labeling were also sometimes seen in these neurons (Fig. 1*B*).

In aspiny and spiny somata, NT-immunogold particles appeared to be distributed randomly over the cytoplasm and nuclei (Fig. 1). The gold particles were, however, often detected near, but not over, the nucleolus (Fig. 1*A*) and were occasionally more discretely localized on nuclear and mitochondrial membranes. In somata and proximal dendrites of spiny neurons, NT-immunogold particles were also seen on or near cytoplasmic tubulovesicles, resembling smooth endoplasmic reticulum, and neurotubules. These labeled organelles were often located near prominent lipofuscin granules (Fig. 1*B*).

Intense peroxidase labeling for NT was localized to discrete segments of the plasma membranes and the membranes of nearby mitochondria in large dendrites, some of which gave rise to spines that were recognizable within the plane of section (Fig. 2*A*). Other large dendrites also showed NT immunoreactivity associated with endosome-like organelles (Fig. 2*B*). In some cases, NT-peroxidase labeling was localized within and near selective asymmetric synaptic specializations in small dendrites (Fig. 2*C*) and dendritic spines (Fig. 2*D*). In dendrites, the peroxidase reaction product was also occasionally seen on membranes of nearby mitochondria and tubulovesicles. The localization of NT to postsynaptic densities and mitochondrial membranes in spiny dendrites was confirmed by immunogold labeling (Fig. 3*A*). In sections that were processed for dual labeling, cNOS was shown to be present in some of the afferents forming symmetric synapses on NT-containing dendrites (Fig. 3*B*).

Axons and axon terminals

NT-LI was seen in a few initial segments of axons and in many small unmyelinated axons in the CPN. The initial segments of axons were recognized by their plasmalemmal undercoating of dense material (Peters et al., 1991) (Fig. 4*A*). In these axons, NT-LI was not uniformly distributed and appeared aggregate over structures resembling neurotubules near mitochondrial

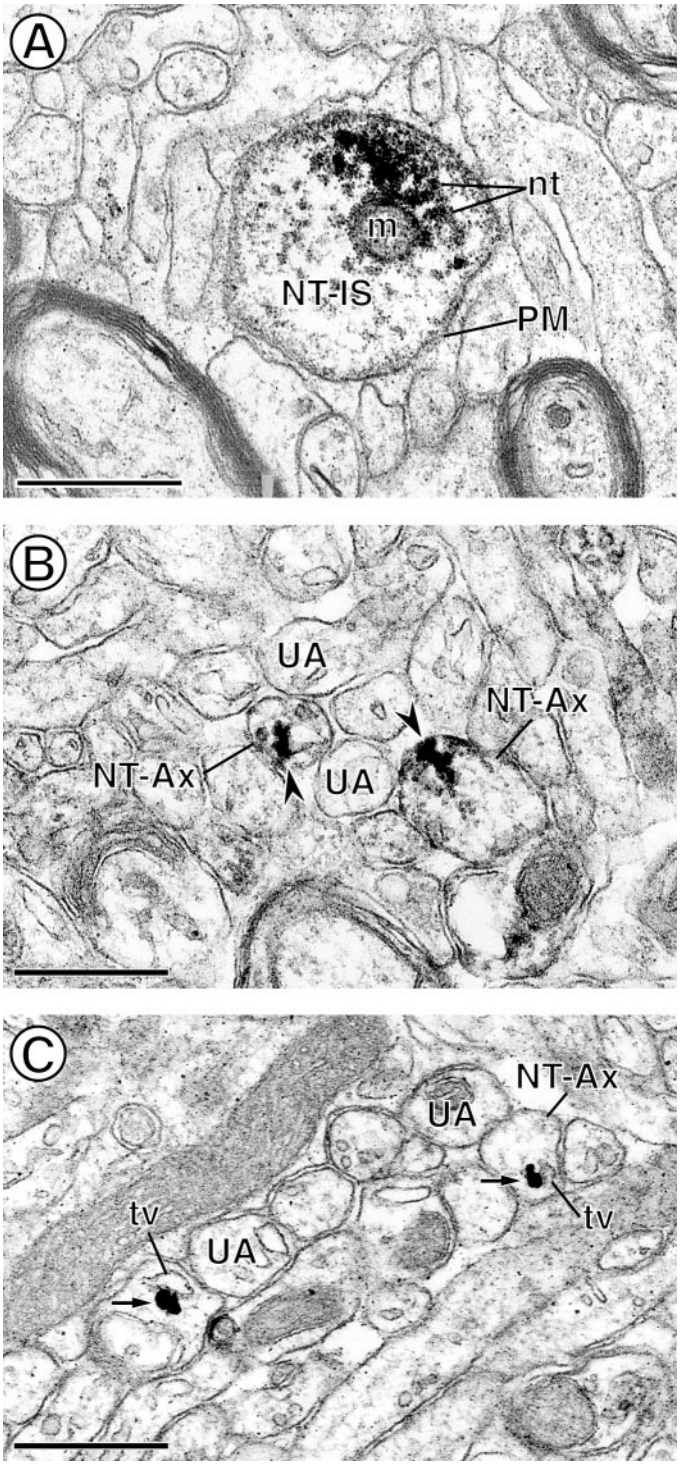

Figure 4. Electron micrographs showing axonal localization of NT. *A*, In the CPN, the immunoperoxidase reaction product is seen in a coronally sectioned initial segment of an axon (*NT-IS*) identified by the dense undercoating of the plasma membrane (*PM*). The labeling is distributed primarily in the region near a mitochondrion (*m*) and overlying presumed neurotubules (*nt*). *B*, In the globus pallidus, immunoperoxidase NT labeling (*arrowheads*) is seen in transversely sectioned small unmyelinated axons (*NT-Ax*) that are located near other unlabeled small axons (*UA*). *C*, In the globus pallidus, NT-immunogold particles (*arrows*) are localized to tubulovesicles (*tv*) within small axons (*NT-Ax*) adjacent to unlabeled axons (*UA*). Scale bars, 0.5 μm.

membranes (Fig. 4*A*). Small unmyelinated axons containing NT-peroxidase labeling were prevalent in the CPN (Figs. 2*D,* 5*A*), as well as in the globus pallidus (Fig. 4*B*). The peroxidase reaction product obscured subcellular organelles, although the labeling often appeared eccentrically located in structures that were shown by immunogold labeling to be tubulovesicular organelles (Fig. 4*C*).

In the CPN, axon terminals containing NT-LI formed mainly asymmetric axospinous synapses as seen by the use of either immunoperoxidase (Fig. 5*A–C*) or immunogold (Fig. 5*D*) labeling methods. These terminals were highly selective and often seen in a neuropil containing many similar terminals without detectable NT immunoreactivity. Occasionally, these NT-labeled terminals were near other small axon terminals showing appositions or symmetric synapses with dendritic spines (Fig. 5*A*). In less intensely labeled axon terminals, the peroxidase NT reaction product was more selectively localized to segments of the plasma membrane and membranes of nearby SSVs (Fig. 5*C*). Many of these also contained mitochondria within the same plane of section. The labeled portions of the plasma membrane apposed unlabeled small axons and axon terminals (Fig. 5*B*) and unlabeled dendrites (Fig. 5*C*). In one example, the unlabeled dendrite also apposed another neuronal process showing an accumulation of NT near the plasma membrane (Fig. 5*C*). In axon terminals, gold particles also were seen near extrasynaptic portions of the plasma membrane (Fig. 5*D*) or were more diffusely distributed within the axoplasm containing abundant SSVs. Labeling for cNOS was present in nearby neuronal processes, the majority of which were without detectable NT-LI (Fig. 5*D*).

Cellular distribution of NT in the globus pallidus

Axons and axon terminals

As discussed above, NT-LI was seen in many small unmyelinated axons in the globus pallidus (Figs. 4*B,C,* 6*A,B*). The most noticeable labeling was, however, seen in axon terminals contacting other axons, dendrites, or glia (Figs. 6, 7). These terminals were most often apposed to unlabeled axon terminals, irrespective of whether a common dendritic target could be seen within the plane of section (Fig. 6). In some cases, the unlabeled terminals were indented around NT-immunoreactive terminals, thus increasing the length of their apposed plasma membranes (Fig. 6*B*). NT-LI was either diffusely distributed within the axoplasm or aggregated near the cytoplasmic surfaces of the plasma membrane. The plasmalemmal labeling was near vesicles or tubulovesicles, having larger diameters than those of the more prevalent SSVs (Fig. 6*C*). Discrete labeling was also seen on the membranes of larger tubulovesicles resembling saccules of smooth endoplasmic reticulum and on mitochondrial membranes in terminals that contained these organelles within the plane of section (Fig. 6*A*).

The dendritic targets of NT-immunoreactive terminals received convergent input from other unlabeled axon terminals and were also often contacted by more than one NT-labeled terminal (Figs. 6*A*, 7*A*). When synaptic specializations were recognizable, most of the NT-labeled and unlabeled terminals formed symmetric synapses. A few afferent inputs to the target dendrites, however, formed synapses with thickened postsynaptic membrane specializations typical of asymmetric synapses. These included terminals containing cNOS immunoreactivity (Fig. 7*A*). The cNOS-containing terminals in this region formed almost exclusively asymmetric axodendritic synapses (Fig. 7) and only occasionally showed discrete vesicular labeling for NT (Fig. 7*B*). The

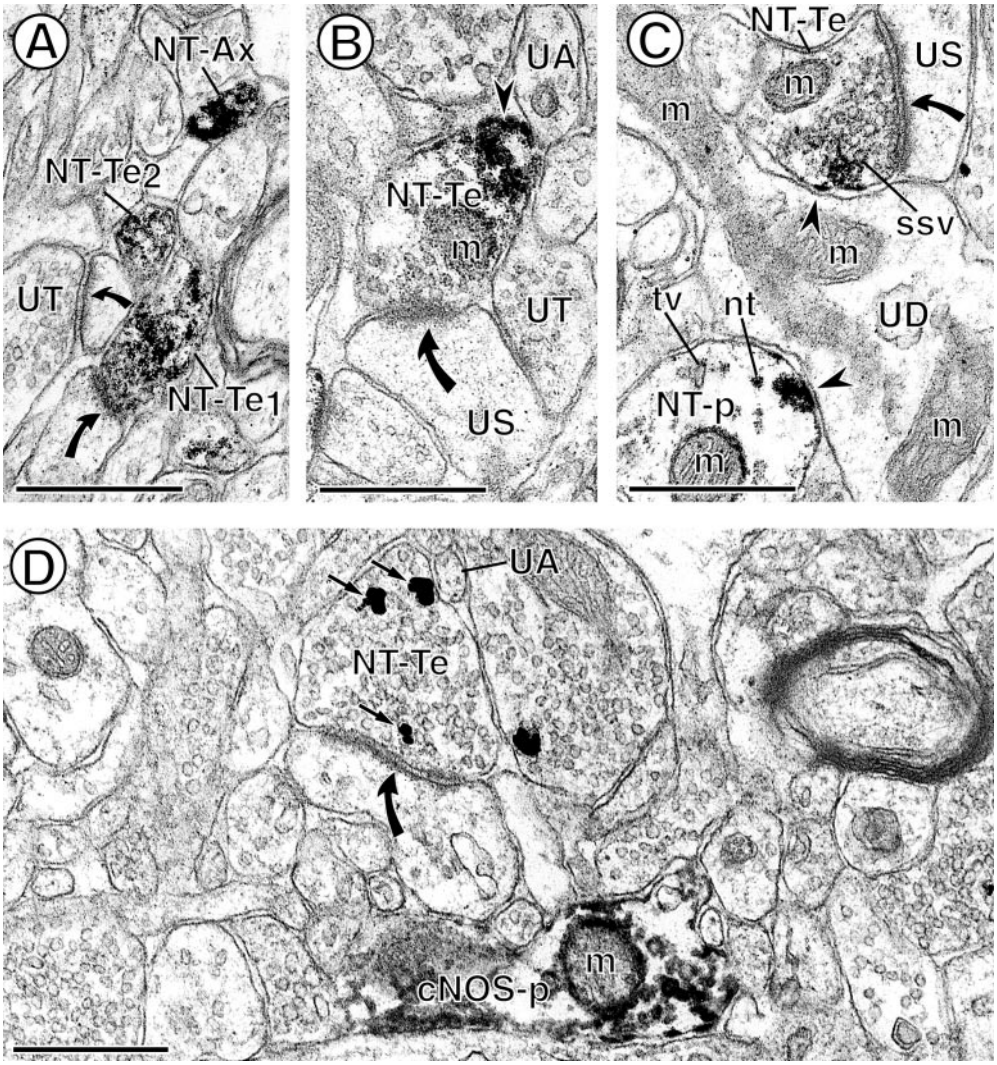

Figure 5. Localizaton of NT to axon terminals forming asymmetric axospinous synapses in the CPN. *A*, Immunoperoxidase NT labeling is seen in an axon terminal (*NT-Te*$_1$) that forms an asymmetric synapse (*bottom curved arrow*) with an unlabeled dendritic spine. An adjacent spine receives a similar synapse (*top curved arrow*) from an unlabeled terminal (*UT*) and is apposed to a small NT-labeled terminal (*NT-Te*$_2$). A small axon (*NT-Ax*) in the neuropil also shows dense NT-peroxidase labeling. *B*, *C*, Immunoperoxidase NT-LI is localized to more discrete portions of the plasma membranes (*arrowhead*) and nearby membranes of small synaptic vesicles (*ssv*) in axon terminals (*NT-Te*) forming asymmetric synapses (*curved arrows*) with unlabeled dendritic spines (*US*). The NT-immunoreactive terminal is apposed to unlabeled axons (*UA*) and terminals (*UT*) in *B* and to an unlabeled dendrite (*UD*) in *C*. The unlabeled dendrite in *C* also apposes a neuronal process (*NT-p*) showing an accumulation of peroxidase reaction product (*arrowhead*) on the plasma membrane and associated with presumed neurotubules (*nt*) and mitochondrial membranes. All labeled profiles in *B* and *C* contain a single mitochondrion (*m*), whereas the apposed dendrite in *C* contains several mitochondria. *D*, Immunogold NT is localized to an axon terminal (*NT-Te*) forming an asymmetric synapse (*large curved arrow*) with an unlabeled dendritic spine. The spine is apposed to a neuronal process containing cNOS-immunoperoxidase labeling (*cNOS-p*) and a mitochondrion (*m*). Scale bars, 0.5 μm.

dendrites postsynaptic to cNOS-containing terminals were usually without detectable NT labeling in single coronal sections, although in longitudinal sections NT-LI was seen in some of the dendritic targets (Fig. 7*C*).

Dendrites and somata

Dendrites and isolated somata in the globus pallidus contained NT-LI. In dendrites, the labeling was mainly associated with mitochondrial membranes and tubulovesicles resembling smooth endoplasmic reticulum (Fig. 7*C*). In somata, immunogold NT labeling, like that in the CPN, was distributed over both the cytoplasm and nuclei, exclusive of the nucleolus. These somata contained prominent lipofuscin granules comparable with those seen in spiny neurons of the CPN.

Astrocytes

NT-LI was prominently displayed within proximal and distal processes of glia in the CPN (Fig. 8*A,B*) and in the globus pallidus (Fig. 8*C,D*). In proximal and distal glial processes in each region, NT labeling was localized to portions of the plasma membrane apposed to unlabeled axon terminals. Thin glial leaflets, showing plasmalemmal NT-LI, were apposed to unlabeled terminals forming mainly asymmetric axospinous synapses in the CPN (Fig. 8*B*) but to those forming symmetric synapses in the globus pallidus (Fig. 8*D*). The small glial processes usually did not contain mitochondria or intermediate glial filaments, as were seen in larger NT-labeled astrocytic processes in the CPN (Fig. 8*A*) and in the globus pallidus (Fig. 8*C*). In larger astrocytic processes, mitochondrial membranes, smooth endoplasmic reticulum, and endosome-like organelles also showed NT-LI (Fig. 8*A*).

DISCUSSION

We have shown that in normal rat brain NT-LI is present in aspiny cNOS-containing neurons in the CPN and in certain spiny neurons, potentially giving rise to NT-labeled inhibitory-type axon terminals in the globus pallidus. The dendrites and putative terminals of spiny neurons were often in contact with cNOS-containing terminals in each of the respective regions. These observations, together with the selective subcellular distribution of NT in spiny and aspiny striatal neurons and glia as well as in excitatory afferents to the CPN, are discussed with respect to their potential involvement in NO-induced intracellular signaling in the basal ganglia.

Methodological considerations

We have referred to the NT labeling as NT-LI to acknowledge potential recognition of closely related products. We believe, however, that the NT antiserum selectively recognizes NT resi-

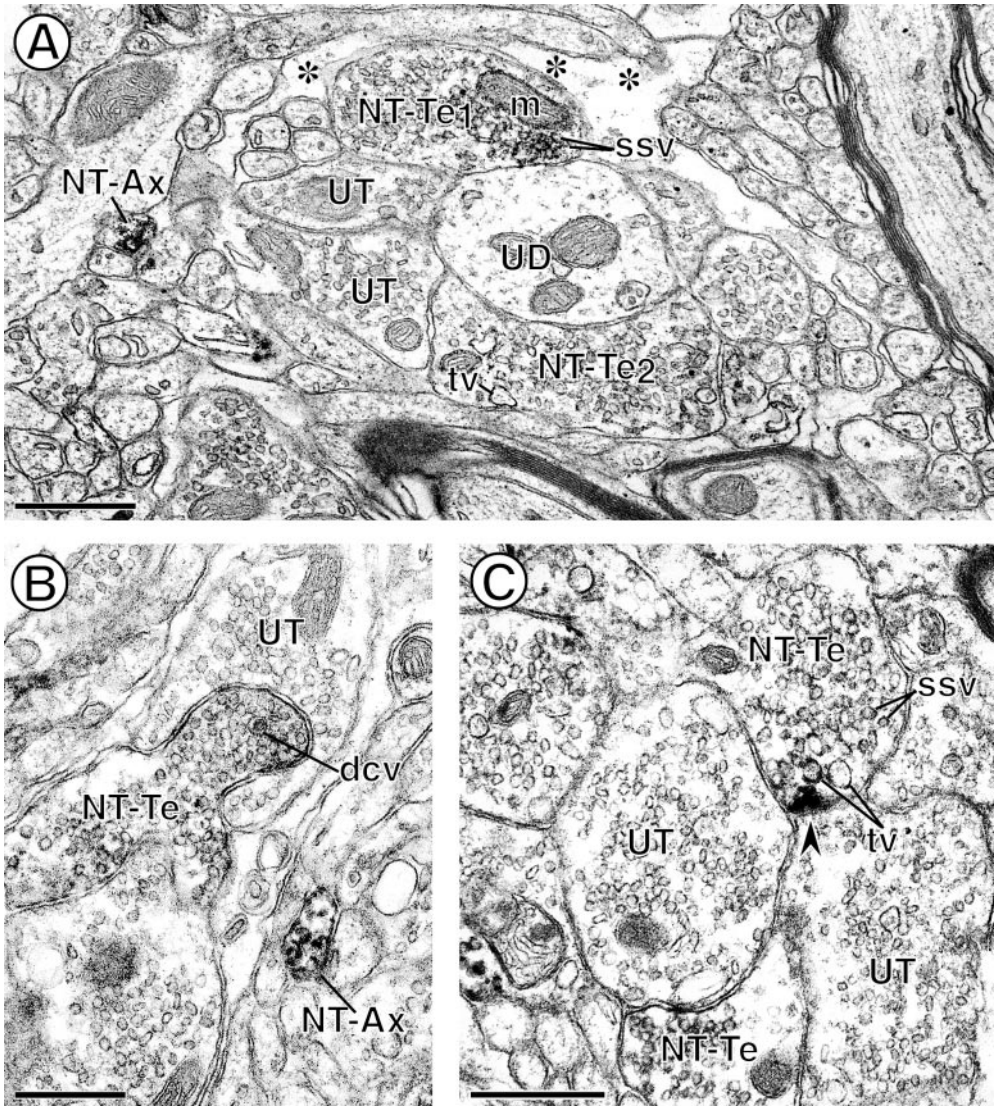

Figure 6. Immunoperoxidase labeling for NT in axon terminals in the globus pallidus. *A*, NT-labeled terminals (*NT-Te*$_1$, *NT-Te*$_2$) converge on an unlabeled dendrite (*UD*) that is also contacted by unlabeled axon terminals (*UT*) and by an unlabeled glial process (*). The peroxidase NT labeling is diffusely distributed around membranes of SSVs (*ssv*) near a mitochondrion (*m*). *B*, *C*, NT-labeled terminals (*NT-Te*) appose unlabeled terminals (*UT*). In *B*, the immunoreactivity is diffusely distributed in the cytoplasm around SSVs and one dense core vesicle (*dcv*). In *C*, the labeling is more discretely aggregated (*arrowhead*) on the cytoplasmic surface of the plasma membrane and along membranes of nearby tubulovesicles (*tv*) and/or SSVs (*ssv*). Small axons in *A* and *B* also contain peroxidase immunoreactivity for NT (*NT-Ax*). Scale bars, 0.5 μm.

dues on the basis of several lines of evidence. It has been demonstrated by immunoblot analysis that the NT antiserum, prepared against nitrated keyhole limpet hemocyanin, is selective for NT residues. No cross-reactivity to tyrosine, phosphotyrosine, aminotyrosine, 3,5-dinitrotyrosine, or *S*-nitroso-cysteine residues was seen (Trifiletti et al., 1995a). Preadsorption of the immune serum with nitrated BSA and 3-nitrotyrosine greatly reduced the intensity of the immunoreaction product in both tissue sections and immunoblots (Beckman et al., 1994; Trifiletti et al., 1995a,b). Despite this specificity, it is most likely that more than one nitroprotein was identified in the present study, because two-dimensional gel analysis separates many different nitroproteins in normal brain homogenates (Beckman et al., 1994).

There are at least six molecular species of cNOS mRNA that are expressed in tissue (Brenman et al., 1997). The antiserum against cNOS that was used in the present study recognizes the major isoforms of cNOS in brain and several other tissues but also may recognize other isoforms (Coers et al., 1998; Laine and De Montellano, 1998; Rothe et al., 1998). The partial recognition of other isoforms could account for our occasional detection of patches of cNOS immunoreactivity in spiny striatal neurons containing NT immunoreactivity, because only aspiny neurons are reported as containing cNOS in the CPN (Nisbet et al., 1994).

Subcellular distribution of NT

NT-LI was densely distributed along outer mitochondrial membranes near the plasmalemma in dendrites and in axon terminals that contained these organelles. Furthermore, oxidants and glutamate receptor activation can alter mitochondrial membrane potential in forebrain neurons (Scanlon and Reynolds, 1998). One or both factors may contribute to the local formation of NT in cytoplasmic regions near mitochondria (Meulemans, 1994; Brorson et al., 1999; Chakraborti et al., 1999). Liposome fusion to mitochondria may also account for the prevalence of lipofuscin granules (Camici and Corazzi, 1997) that were seen in many of the NT-labeled somata in the present study. In addition, however, we observed NT-LI within the cytosol, along membranes of tubulovesicles or smooth endoplasmic reticulum in dendrites, and in association with these organelles, as well as membranes of synaptic vesicles in axon terminals. This subcellular distribution may reflect NT incorporation into the C terminal of α tubulin (Eiserich et al., 1999), because tyrosinated α tubulin is present in the cytosol and associated with membranes including those of the smooth endoplasmic reticulum and other organelles showing NT labeling in the present study (Strocchi et al., 1981; Beltramo et al., 1992). In both dendrites and axons, the tubulin-associated or-

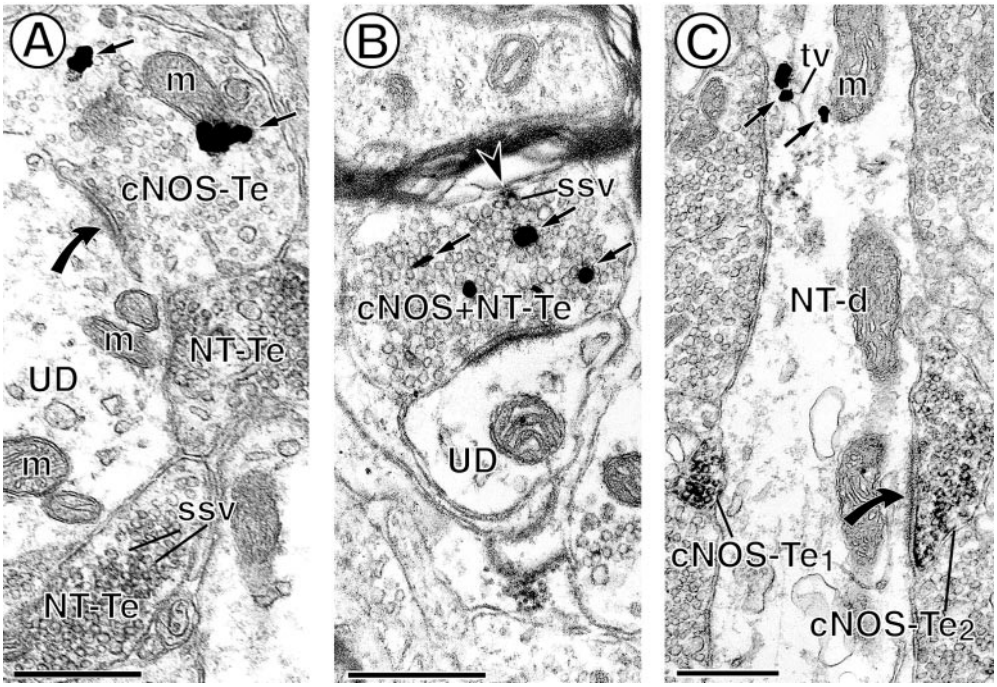

Figure 7. Dual labeling for NT and cNOS in the globus pallidus. *A*, Immunoperoxidase labeling of NT is seen in two axon terminals (*NT-Te*) contacting a coronally sectioned unlabeled dendrite (*UD*). Within these axon terminals, the NT-peroxidase reaction product is diffusely distributed around membranes of small synaptic vesicles (*ssv*). The dendrite also receives an asymmetric synapse (*large curved arrow*) from an axon terminal that contains immunogold labeling for cNOS (*cNOS-Te*). One cluster of cNOS gold particles is seen near the outer membrane of a mitochondrion (*m*). Other mitochondria (*m*) are present in the unlabeled dendrite beneath the NT-labeled terminals. *B*, Immunoperoxidase labeling for NT (*arrowhead*) is discretely localized to the membranes of a few SSVs (*ssv*) near the plasma membrane in an axon terminal that contains immunogold labeling (*small arrows*) for cNOS (*cNOS + NT-Te*). This terminal forms an asymmetric synapse (*large curved arrow*) with a coronally sectioned unlabeled dendrite (*UD*). *C*, Reversal of the markers shows immunoperoxidase localization of cNOS in axon terminals ($cNOS\text{-}Te_1$, $cNOS\text{-}Te_2$) that appose or form, respectively, an asymmetric synapse (*large curved arrow*) with a common dendrite containing immunogold (*small arrows*) NT (*NT-d*). The gold particles are distributed along membranes of tubulovesicles (*tv*) resembling smooth endoplasmic reticulum and a mitochondrion (*m*). Scale bars, 0.5 μm.

ganelles, particularly the smooth endoplasmic reticulum, are involved in antioxidant-sensitive axonal transport of macromolecules (Southam et al., 1991).

We observed NT labeling in selective neuronal nuclei, suggesting that NT products formed by free radicals may be involved in gene regulation (Yun et al., 1998; Briski, 1999). The cytoplasmic and nuclear distribution of NT may also reflect sites where oxidants play a role in increasing cytosolic calcium via release from cellular storage organelles (Suzuki et al., 1997). Similarly, our localization of NT at asymmetric synapses of the type formed by glutamatergic terminals on dendrites and dendritic spines in the CPN is consistent with localization to sites where oxidants may increase the permeability of calcium channels, including those of the NMDA subtype of glutamate receptor (Price et al., 1993). The involvement of glutamatergic transmission in the genesis of NT is supported by the high density of asymmetric, excitatory-type synapses as compared with symmetric synapses in the CPN (Gerfen, 1988; Rodriguez and Pickel, 1999). Although symmetric synapses predominate in the globus pallidus, terminals forming asymmetric junctions are also present in this region (DiFiglia and Rafols, 1988) and provide a potential source of glutamate (Hanson and Smith, 1999)

The oxidants involved in the production of NT also may include free radical metabolites of dopamine (Berman and Hastings, 1999), which is one of the major neurotransmitters in afferents to the CPN and in axons passing through the globus pallidus (Bjorklund and Lindvall, 1984). This idea is supported by studies showing that glutamate-induced pruning of dendritic spines is stabilized by antioxidants and by dopamine D2 receptor activation (Smythies, 1999).

A role for NT in oxidant-stimulated signal transduction involving calcium-permeable channels in the plasma membrane is also supported by our localization of NT to the plasma membrane of astrocytic processes near axon terminals, because reactive oxygen species and calcium have been implicated in neuroglial signaling (Conti et al., 1997; Matsutani and Yamamoto, 1997; Atkins and Sweatt, 1999). Furthermore, we have shown that intermediate filaments typical of astrocytes are present in many of the NT-labeled glial processes, and NO donors are known to induce tyrosine nitration in astrocytes as well as in neurons (Bonfoco et al., 1996).

NT localization in aspiny and spiny neurons in the CPN

The present localization of NT in cNOS-containing aspiny neurons is consistent with the idea that protein nitration in these cells is indirectly attributed to locally synthesized NO or NO-related species requiring an influx of extracellular calcium, mainly through NMDA receptors that are prevalent in aspiny neurons (Price et al., 1993). Aspiny interneurons containing GABA are those that appear most markedly influenced by NMDA receptor activation (Sadikot et al., 1998). Thus, the production of NT may play a particularly important role in the modulatory actions of NO and/or glutamate on the output of this population of interneurons. The presence of NT mainly in the somata and proximal dendrites of cNOS-immunoreactive neurons also supports the conclusion that the nitrated proteins are minimally transported into the distal dendrites or terminals of interneurons, as most likely occurs in spiny projection neurons.

Selective spiny neurons in the CPN and a few neurons in the globus pallidus also contained NT, but little or no cNOS, immunoreactivity. These neurons are morphologically similar to those identified as containing GABA (Gritti et al., 1993). In addition, some of the presently observed NT-labeled dendrites in the CPN and globus pallidus received synaptic input from cNOS-immunoreactive terminals. These terminals, or nearby cNOS-containing dendrites, are likely to be the major source of NO.

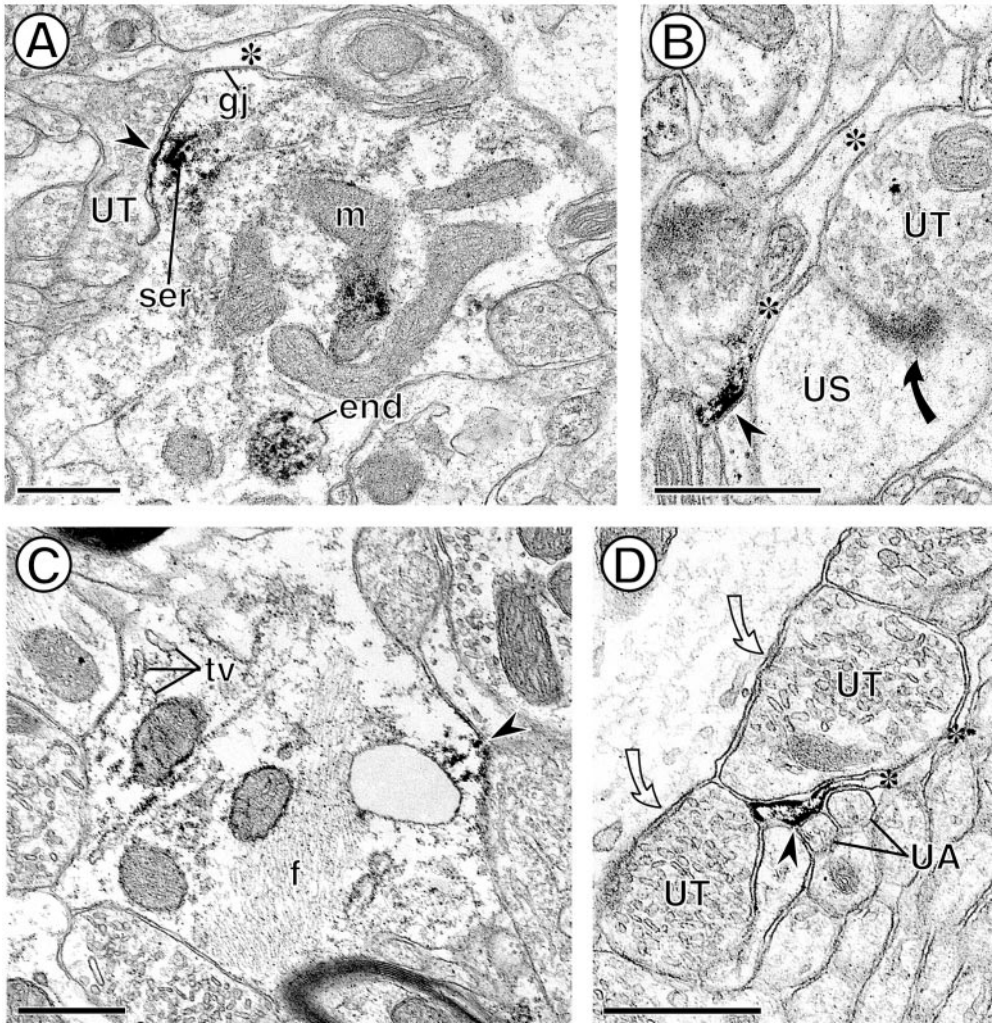

Figure 8. Electron micrograph showing immunoperoxidase NT labeling in a glial process in the CPN (*A, B*) and the globus pallidus (*C, D*). *A*, The reaction product (*arrowhead*) is seen along portions of the plasma membrane of an astrocytic process apposed to an unlabeled terminal (*UT*). The labeling is also localized to membranes of nearby smooth endoplasmic reticulum (*ser*), an endosome (*end*), and a mitochondrion (*m*). The labeled process has a gap junction (*gj*) with a smaller unlabeled glial process (*). *B*, NT-LI is localized mainly to the plasma membrane (*arrowhead*) in the distal tip of a glial process that is in continuity with unlabeled portions of the same profile (*). The glial process is apposed to an unlabeled terminal (*UT*) that forms an asymmetric synapse (*curved arrow*) with an unlabeled dendritic spine (*US*). *C*, Peroxidase NT-LI is seen along portions of the plasma membrane (*arrowhead*) and along membranes of tubulovesicles (*tv*) and mitochondria in an astrocytic process containing abundant filaments (*f*). *D*, Peroxidase labeling (*arrowhead*) is seen along the plasmalemma of a glial process in continuity with other unlabeled portions of the same profile (*). The labeled glial process is apposed to unlabeled terminals (*UT*) forming symmetric synapses (*curved arrows*) and to unlabeled axons (*UA*). Scale bars, 0.5 μm.

Axonal distribution of NT

We found NT-LI in a few axon initial segments in the CPN and in many small unmyelinated axons and axon terminals forming asymmetric synapses in the CPN or symmetric synapses in the globus pallidus. Those terminals forming asymmetric synapses in the CPN are known to be primarily glutamatergic, and peroxynitrite, the likely agent for NT formation (Ischiropoulos et al., 1992), inhibits the glutamate transporter (Volterra et al., 1992, 1994; Trotti et al., 1996). In addition, NO has also been implicated in regulating the dopamine transporter in the striatum (Chaparro-Huerta et al., 1997), which may be reflected in our localization of NT to small axon terminals apposing or forming symmetric synapses with dendritic spines in a manner described for dopaminergic (Nirenberg et al., 1996) as well as cholinergic terminals in the CPN (DiFiglia, 1987).

In both the CPN and globus pallidus, our selective localization of NT in axon terminals may also reflect sites where NO and hydroxyl radicals modulate neurotransmitter release evoked by activation of calcium-permeable glutamate receptors (Montague et al., 1994; Ohkuma et al., 1998). The retrograde transport of NT proteins to somata might account for the observed labeling of NT in many small axons in the globus pallidus and CPN. We cannot, however, exclude the possibility that the NT proteins are generated in somata or dendrites in the CPN and transported along with other proteins to axon terminals in the globus pallidus. This question and others regarding the role of NT in normal motor function and in the pathogenesis of motor disorders such as Huntington's disease that affects striatopallidal neurons (Dawson and Dawson, 1996; Palfi et al., 1996) require further investigation.

REFERENCES

Atkins CM, Sweatt JD (1999) Reactive oxygen species mediate activity-dependent neuron-glia signaling in output fibers of the hippocampus. J Neurosci 19:7241–7248.

Beckman JS, Chen J, Ischiropoulous H, Crow JP (1994) Oxidative chemistry of peroxynitrite. Methods Enzymol 233:229–240.

Beltramo DM, Alonso AC, Barra HS (1992) Tyrosinated, detyrosinated and acetylated tubulin isotypes in rat brain membranes. Their proportions in comparison with those in cytosol. Mol Cell Biochem 112:173–180.

Berman SB, Hastings TG (1999) Dopamine oxidation alters mitochondrial respiration and induces permeability transition in brain mitochondria: implications for Parkinson's disease. J Neurochem 73:1127–1137.

Bjorklund A, Lindvall O (1984) Dopamine-containing systems in the CNS. In: Handbook of chemical neuroanatomy, Vol 2, Classical transmitters in the CNS, Pt I (Bjorklund A, Hokfelt T, eds), pp 55–121. Amsterdam: Elsevier.

Bonfoco E, Leist M, Zhivotovsky B, Orrenius S, Lipton SA, Nicotera P (1996) Cytoskeletal breakdown and apoptosis elicited by NO donors in

cerebellar granule cells require NMDA receptor activation. J Neurochem 67:2484–2493.
Bredt DS, Glatt CE, Hwang PM, Fotuhi M, Dawson TM, Snyder SH (1991) Nitric oxide synthase protein and mRNA are discretely localized in neuronal populations of the mammalian CNS together with NADPH diaphorase. Neuron 7:615–624.
Brenman JE, Xia HH, Chao DS, Black SM, Bredt DS (1997) Regulation of neuronal nitric oxide synthase through alternative transcripts. Dev Neurosci 19:224–231.
Briski KP (1999) Pharmacological manipulation of central nitric oxide/guanylate cyclase activity alters Fos expression by rat hypothalamic vasopressinergic neurons during acute glucose deprivation. J Chem Neuroanat 17:13–19.
Brorson JR, Schumacker PT, Zhang H (1999) Nitric oxide acutely inhibits neuronal energy production. J Neurosci 19:147–158.
Camici O, Corazzi L (1997) Phosphatidylserine translocation into brain mitochondria: involvement of a fusogenic protein associated with mitochondrial membranes. Mol Cell Biochem 175:71–80.
Chakraborti T, Mondal M, Roychoudhury S, Chakraborti S (1999) Oxidant, mitochondria and calcium: an overview. Cell Signal 11:77–85.
Chan J, Aoki C, Pickel VM (1990) Optimization of differential immunogold-silver and peroxidase labeling with maintenance of ultrastructure in brain sections before plastic embedding. J Neurosci Methods 33:113–127.
Chaparro-Huerta V, Beas-Zárate C, Guerrero MU, Feria-Velasco A (1997) Nitric oxide involvement in regulating the dopamine transport in the striatal region of rat brain. Neurochem Int 31:607–616.
Coers W, Timens W, Kempinga C, Klok PA, Moshage H (1998) Specificity of antibodies to nitric oxide synthase isoforms in human, guinea pig, rat, and mouse tissues. J Histochem Cytochem 46:1385–1392.
Conti F, Minelli A, DeBiasi S, Melone M (1997) Neuronal and glial localization of NMDA receptors in the cerebral cortex. Mol Neurobiol 14:1–18.
Crow JP, Ischiropoulos H (1996) Detection and quantitation of nitrotyrosine residues in proteins: *in vivo* marker of peroxynitrite. Methods Enzymol 269:185–194.
Dalton TD, Shertzer HG, Puga A (1999) Regulation of gene expression by reactive oxygen. Annu Rev Pharmacol Toxicol 39:67–101.
Dawson TM, Bredt DS, Fotuhi M, Hwang PM, Snyder SH (1991) Nitric oxide synthase and neuronal NADPH diaphorase are identical in brain and peripheral tissues. Proc Natl Acad Sci USA 88:7797–7801.
Dawson VL, Dawson TM (1996) Nitric oxide neurotoxicity. J Chem Neuroanat 10:179–190.
DiFiglia M (1987) Synaptic organization of cholinergic neurons in the monkey neostriatum. J Comp Neurol 255:245–258.
DiFiglia M, Rafols JA (1988) Synaptic organization of the globus pallidus. J Electron Microsc Tech 10:247–263.
DiFiglia M, Pasik T, Pasik P (1980) Ultrastructure of Golgi-impregnated and gold-toned spiny and aspiny neurons in the monkey neostriatum. J Neurocytol 9:471–492.
Eiserich JP, Estevez AG, Bamberg TV, Ye YZ, Chumley PH, Beckman JS, Freeman BA (1999) Microtubule dysfunction by posttranslational nitrotyrosination of alpha-tubulin: a nitric oxide-dependent mechanism of cellular injury. Proc Natl Acad Sci USA 96:6365–6370.
Gerfen CR (1988) Synaptic organization of the striatum. J Electron Microsc Tech 10:265–281.
Gracy KN, Pickel VM (1997) Ultrastructural localization and comparative distribution of nitric oxide synthase and *N*-methyl-D-aspartate receptors in the shell of the rat nucleus accumbens. Brain Res 747:259–272.
Gritti I, Mainville L, Jones BE (1993) Codistribution of GABA- with acetylcholine-synthesizing neurons in the basal forebrain of the rat. J Comp Neurol 329:438–457.
Hanson JE, Smith Y (1999) Group I metabotropic glutamate receptors at GABAergic synapses in monkeys. J Neurosci 19:6488–6496.
Ischiropoulos H, Zhu L, Chen J, Tsai M, Martin JC, Smith CD, Beckman JS (1992) Peroxynitrite-mediated tyrosine nitration catalyzed by superoxide dismutase. Arch Biochem Biophys 298:431–437.
Ischiropoulos H, Beers MF, Ohnishi ST, Fisher D, Garner SE, Thom SR (1996) Nitric oxide production and perivascular tyrosine nitration in brain after carbon monoxide poisoning in the rat. J Clin Invest 97:2260–2267.
King JC, Lechan RM, Kugel G, Anthony ELP (1983) Acrolein: a fixative for immunocytochemical localization of peptides in the central nervous system. J Histochem Cytochem 31:62–68.
Laine R, De Montellano PR (1998) Neuronal nitric oxide synthase isoforms alpha and mu are closely related calpain-sensitive proteins. Mol Pharmacol 54:305–312.
Leranth C, Pickel VM (1989) Electron microscopic pre-embedding double immunostaining methods. In: Neuroanatomical tract-tracing methods 2: recent progress (Heimer L, Zaborszky L, eds), pp 129–172. New York: Plenum.
Matsutani S, Yamamoto N (1997) Neuronal regulation of astrocyte morphology in vitro is mediated by GABAergic signaling. Glia 20:1–9.
Meulemans A (1994) Diffusion coefficients and half-lives of nitric oxide and *N*-nitroso-L-arginine in rat cortex. Neurosci Lett 171:89–93.
Montague PR, Gancayco CD, Winn MJ, Marchase RB, Friedlander MJ (1994) Role of NO production in NMDA receptor-mediated neurotransmitter release in cerebral cortex. Science 263:973–977.
Nirenberg MJ, Vaughan RA, Uhl GR, Kuhar MJ, Pickel VM (1996) The dopamine transporter is localized to dendritic and axonal plasma membranes of nigrostriatal dopaminergic neurons. J Neurosci 16:436–447.
Nisbet AP, Foster OJF, Kingsbury A, Lees AJ, Marsden CD (1994) Nitric oxide synthase mRNA expression in human subthalamic nucleus, striatum and globus pallidus: implications for basal ganglia function. Mol Brain Res 22:329–332.
Ohkuma SO, Katsura M, Hibino T, Hara A, Shirotani K, Ishikawa E, Kuriyama K (1998) Mechanisms for facilitation of nitric oxide-evoked [^{3}H]GABA release by removal of hydroxyl radical. J Neurochem 71:1501–1510.
Ohshima H, Friesen M, Brouet I, Bartsch H (1990) Nitrotyrosine as a new marker for endogenous nitrosation and nitration of proteins. Food Chem Toxicol 28:647–652.
Palfi SP, Ferrante RJ, Brouillet E, Beal MF, Dolan R, Guyot MC, Peschanski M, Hantraye P (1996) Chronic 3-nitropropionic acid treatment in baboons replicates the cognitive and motor deficits of Huntington's disease. J Neurosci 16:3019–3025.
Paxinos G, Watson C (1986) The rat brain in stereotaxic coordinates. New York: Academic.
Peters A, Palay SL, Webster HD (1991) The fine structure of the nervous system. New York: Oxford UP.
Pickel VM, Pohorille A, Chan J, Tate SS, Nirenberg MJ (1999) Regional and subcellular distribution of a neutral and basic amino acid transporter in forebrain neurons containing nitric oxide synthase. J Comp Neurol 404:459–472.
Price Jr RH, Mayer B, Beitz AJ (1993) Nitric oxide synthase neurons in rat brain express more NMDA receptor mRNA than non-NOS neurons. NeuroReport 4:807–810.
Reynolds ES (1963) The use of lead citrate at high pH as an electron-opaque stain in electron microscopy. J Cell Biol 17:208.
Rodriguez JJ, Pickel VM (1999) Enhancement of *N*-methyl-D-aspartate (NMDA) immunoreactivity in residual dendritic spines in the caudate-putamen nucleus after chronic haloperidol administration. Synapse 33:289–303.
Rothe F, Canzler U, Wolf G (1998) Subcellular localization of the neuronal isoform of nitric oxide synthase in the rat brain: a critical evaluation. Neuroscience 83:259–269.
Sadikot AF, Burhan AM, Belanger MC, Sasseville R (1998) NMDA receptor antagonists influence early development of GABAergic interneurons in the mammalian striatum. Dev Brain Res 105:35–42.
Scanlon JM, Reynolds IJ (1998) Effects of oxidants and glutamate receptor activation on mitochondrial membrane potential in rat forebrain neurons. J Neurochem 71:2392–2400.
Smythies J (1999) Redox mechanisms at the glutamate synapse and their significance: a review. Eur J Pharmacol 370:1–7.
Southam E, Thomas PK, King RH, Goss-Sampson MA, Muller DP (1991) Experimental vitamin E deficiency in rats. Morphological and functional evidence of abnormal axonal transport secondary to free radical damage. Brain 114:915–936.
Strocchi P, Brown BA, Young JD, Bonventre JA, Gilbert JM (1981) The characterization of tubulin in CNS membrane fractions. J Neurochem 37:1295–1307.
Suzuki YJ, Forman HJ, Sevanian A (1997) Oxidants as stimulators of signal transduction. Free Radic Biol Med 22:269–285.
Trifiletti RR, Bandele AN, Bolan EA (1995a) Protein tyrosine nitration in the nervous system: a marker of brain nitric oxide production. Soc Neurosci Abstr 21:869.
Trifiletti RR, Bolan EA, Bandele AN (1995b) Protein tyrosine nitra-

tionin the developing nervous system: a marker of brain nitric oxide production. Ann Neurol 38:523.

Trotti D, Rossi D, Gjesdal O, Levy LM, Racagni G, Danbolt NC, Volterra A (1996) Peroxynitrite inhibits glutamate transporter subtypes. J Biol Chem 271:5976–5979.

van der Vliet A, Eiserich JP, O'Neill CA, Halliwell B, Cross CE (1995) Tyrosine modification by reactive nitrogen species: a closer look. Arch Biochem Biophys 319:341–349.

van der Vliet A, Eiserich JP, Kaur H, Cross CE, Halliwell B (1996) Nitrotyrosine as biomarker for reactive nitrogen species. Methods Enzymol 269:175–184.

Volterra A, Trotti D, Cassutti P, Tromba C, Salvaggio A, Melcangi RC, Racagni G (1992) High sensitivity of glutamate uptake to extracellular free arachidonic acid levels in rat cortical synaptosomes and astrocytes. J Neurochem 59:600–606.

Volterra A, Trotti D, Floridi S, Racagni G (1994) Reactive oxygen species inhibit high-affinity glutamate uptake: molecular mechanism and neuropathological implications. Ann NY Acad Sci 738: 153–162.

Ye YZ, Strong M, Huang ZQ, Beckman JS (1996) Antibodies that recognize nitrotyrosine. Methods Enzymol 269:201–209.

Yun HY, Gonzalez-Zulueta M, Dawson VL, Dawson TM (1998) Nitric oxide mediates *N*-methyl-D-aspartate receptor-induced activation of $p21^{ras}$. Proc Natl Acad Sci USA 95:5773–5778.